ISSN (Print) : 2320 – 3765
ISSN (Online): 2278 – 8875

International Journal of Advanced Research in Electrical, Electronics and Instrumentation Engineering

(A High Impact Factor, Monthly, Peer Reviewed Journal)

Website: www.ijareeie.com

Vol. 7, Issue 5, May 2018

A Novel Control Strategy for Improving the Ride through Capability OFVSC-HVDC Transmission System Supplying to Passive Industrial Applications

J.Rajendra[1], G.Veeranjaneyulu[2]

PG Student, Dept. of EEE, RVR & JC College of Engineering, Guntur, Andhra Pradesh, India[1]

Assistant Professor, Dept. of EEE, RVR & JC College of Engineering, Guntur, Andhra Pradesh, India[2]

ABSTRACT:This paper presents a modified current control strategy (MCCS) and a frequency hysteresis control (FHC) for improving the fault ride-through capability of a VSC-HVDC transmission system supplying to passive industrial installations. As the industrial loads are highly delicate to voltage drops than that of the frequency variations, it become difficult to maintain voltage stability during severe faults. Hence the proposed HVDC system offers the operational flexibility in terms of voltage stability in addition with improved ride-through capability of HVDC system. The control mainly involves three stages i.e. firstly the factor that effects the voltage stability has to be determined and secondly as per the determined results, the MCCS is framed so as to improve the ac voltage under transient conditions and finally the FHC is added with MCCS for better control. Hence MCCS combined FHC will improve the ac voltage of the passive system. The simulation tests for single-phase ground and three-phase ground faults are done in MATLAB/PSCAD and the results are analysed.

KEYWORDS: Pulse width modulation, Voltage stability, Passive industrial installations, Modified current control strategy (MCCS), Frequency hysteresis control (FHC), Voltage source converter VSC.

I.INTRODUCTION

The electricity networks of today increasingly need control and stability at high levels of loading. Increasing the stability through adding more lines is not always an option due to restrictions in right-of-way or limits to acceptable short circuit current. In recent years, it has been found to be economical to transmit bulk amounts of power over distances or across water by means of high DC voltage rather than multiphase AC. The new HVDC system known as VSC-HVDC, has Voltage Source Converters and Pulse Width Modulation (PWM) at its core, different from current source converters in traditional HVDC [1, 2]. With the development of industries, voltage sags have become major problem for the stability of industrial systems [3, 4]. These systems are more sensitive to voltage drops compared to frequency deviations [5, 6].Hence, in order to enhance the ride-through capability of system, it is important to maintain voltage stable. With the increased usage of VSC-HVDC systems which is playing an important role in power technology [7, 8].

The VSC-HVDC systems have the capability to control the active and reactive power [9] and feed power into passive networks [10-13]. When a VSC-HVDC link is supplying a passive network, the VSC controller can use the direct current control to suppress fault currents [14]. Due to the faults in the sending side of the VSC-HVDC transmission system, the transferred active power reduces and the dc voltage drops, which results in ac voltage sags at the receiving side [20, 21]. As the industrial loads are more sensitive to voltage drops, that may cause voltage collapse in the passive industrial network [15].

Over the decade, few research efforts have been made to enhance the stability of voltage in passive networks. A new VSC controller supplying passive industrial plants is proposed in [6], where the VSC-HVDC uses the ac voltage

ISSN (Print) : 2320 – 3765
ISSN (Online): 2278 – 8875

International Journal of Advanced Research in Electrical, Electronics and Instrumentation Engineering

(A High Impact Factor, Monthly, Peer Reviewed Journal)

Website: www.ijareeie.com

Vol. 7, Issue 5, May 2018

and frequency control. The designed model gives priority to keeping up the ac voltage and decrease the frequency slightly during faults. Since the controller hasn't set the frequency of the passive network in steady-state operation, the system has failed to start reliably and this control strategy cannot make passive networks ride through severe faults. In [15], a droop frequency controller is developed. The idea is to produce a new reference frequency of the VSC output voltage based on the dc voltage in which the voltage stability is still bad. A Multi-terminal VSC-HVDC system connecting the main grid, wind mills and oil platforms was analysed in [16-18]. The results of this VSC-MTDC system in steady and transient conditions were also presented. The enhanced fault ride-through method for offshore platforms is given in [17]. When faults occur in the offshore oil installations, the control strategy recommended in [17] employs a voltage-dependent limiter, to limit the maximum amount of active power from the offshore VSC. But the main worry of [17] is the dc voltage, but not the ac voltage of industrial applications. In [19], a nonlinear control strategy targeting to improve the performance characteristics of the VSC output voltage was developed in which the ac grid dynamics were not considered [30].

This paper offers novel control strategies for a VSC-HVDC link to enhance the fault ride–through capability of passive industrial installations. The new VSC controller based on the conventional ac voltage control (CAVC) comprises of a modified current control strategy (MCCS) and a frequency hysteresis control (FHC). The control strategies are designed to improve the stability of voltage in passive industrial systems. Effects of metallic single-phase to ground and three-phase to ground faults at the sending end of the VSC-HVDC system are simulated and examined in PSCAD/MATLAB. The overview of this paper is as follows. Section II presents the primary information and designing of the VSC-HVDC system supplying passive industrial loads. The control strategies of the MCCS and FHC are presented in section III. Section IV briefs about the carried simulation tests and the paper conclusion are represented in Section V. The test parameters of the designed system are given in section VI.

II. BASIC CIRCUIT MODEL OF TEST SYSTEM

2.1 System Topology:

It is represented in Fig. 1 [15] that the power is transmitted from the main ac grid to the passive industrial system by VSC-HVDC system. As the most of the industrial loads are induction motors, the study of this paper is mainly concentrates on induction motors. Variable frequency drives and protective functions are excluded in this paper as they are minor part of the passive load [6].

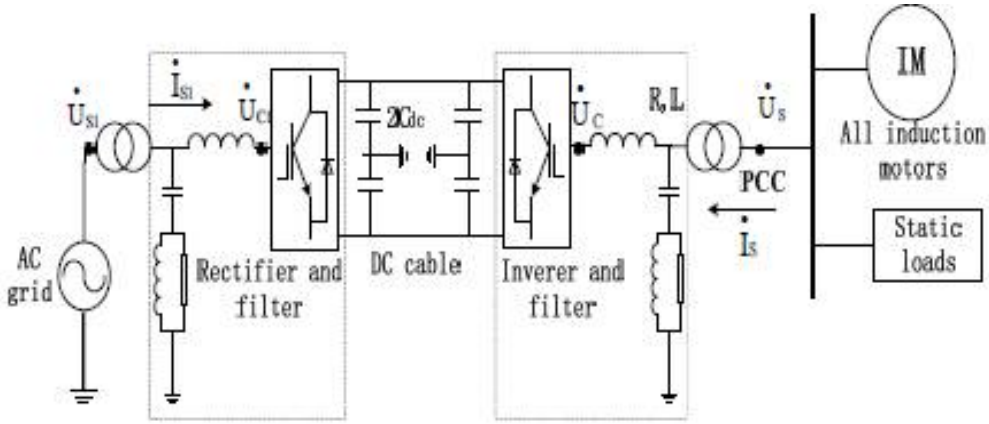

Fig.1.The basic VSC-HVDC system topology

ISSN (Print) : 2320 – 3765
ISSN (Online): 2278 – 8875

International Journal of Advanced Research in Electrical, Electronics and Instrumentation Engineering

(A High Impact Factor, Monthly, Peer Reviewed Journal)

Website: www.ijareeie.com

Vol. 7, Issue 5, May 2018

2.2 Mathematical Model of VSC:

The basic network of the VSC mentioned in [25] is shown in Fig. 2.

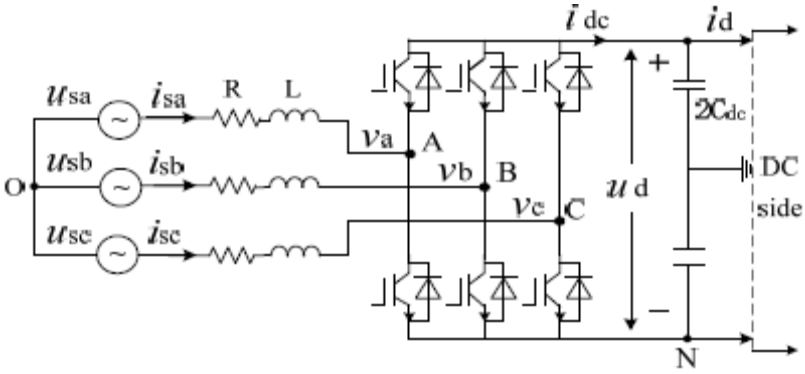

Fig.2.The circuit model of VSC

By applying three-phase Kirchhoff law, the voltage equations are as follows:

$$\begin{cases} L.\frac{di_{sa}}{dt} + R.i_{sa} = u_{sa} - v_a \\ L.\frac{di_{sb}}{dt} + R.i_{sb} = u_{sb} - v_b \\ L.\frac{di_{sc}}{dt} + R.i_{sc} = u_{sc} - v_c \end{cases} \quad (1)$$

After dq –axis transformation:

$$\begin{cases} L.\frac{di_{sd}}{dt} = u_{sd} - v_{sd} + \omega L i_{sq} - R i_{sd} \\ L.\frac{di_{sq}}{dt} = u_{sq} - v_{sq} - \omega L i_{sd} - R i_{sq} \end{cases} \quad (2)$$

The equations in frequency domain, which is presented in the positive and negative sequence, can be acquired by Laplace transformation [26]:

$$\begin{cases} (R + sL).i_{sd}^{+}(s) = u_{sd}^{+}(s) - v_d^{+}(s) + \omega L i_{sq}^{+}(s) \\ (R + sL).i_{sq}^{+}(s) = u_{sq}^{+}(s) - v_q^{+}(s) - \omega L i_{sd}^{+}(s) \end{cases} \quad (3)$$

$$\begin{cases} (R + sL).i_{sd}^{-}(s) = u_{sd}^{-}(s) - v_d^{-}(s) - \omega L i_{sq}^{-}(s) \\ (R + sL).i_{sq}^{-}(s) = u_{sq}^{-}(s) - v_q^{-}(s) + \omega L i_{sd}^{+}(s) \end{cases} \quad (4)$$

ISSN (Print) : 2320 – 3765
ISSN (Online): 2278 – 8875

International Journal of Advanced Research in Electrical, Electronics and Instrumentation Engineering

(A High Impact Factor, Monthly, Peer Reviewed Journal)

Website: www.ijareeie.com

Vol. 7, Issue 5, May 2018

2.3 Overall Control Description of VSC-HVDC:

The control of the VSC-HVDC is done by inner and outer control loop. The main purpose of the VSC inner control loop is to make *dq*-axis current components (i.e., $i_{sd}$and i_{sq}) follow references produced from the outer control loop. So as to suppress negative sequence currents in unbalanced faults, we set the command references as [28].As the VSC-HVDC system transmits power into passive network, the outer control loop of the rectifier station function on the dc voltage control mode and the ac voltage or reactive power control mode. On the grid end, VSC can reach synchronization with the main grid by means of the Phase Locked Loop (PLL) [8, 10].

$$i_{sdref}^{-} = i_{sqref}^{-} = 0 \qquad (5)$$

The control system of the rectifier station [8] is shown in Fig. 3, where *Q* is the reactive power transmitted from ac grid to the rectifier station, *Us1* is the amplitude of the voltage of the ac grid (see Fig. 1), $Q_{ref}$and $U_{s1ref}$are the reference values of *Q* and U_{s1}.

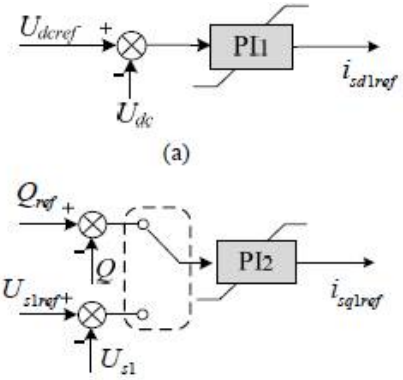

Fig.3.The outer control loop of the rectifier station. (a) dc voltage control mode. (b) ac voltage or reactive power control mode.

The VSC in the receiving side works on the voltage control mode, which is designed to control the ac voltage at the PCC. The control system is illustrated in Fig. 4. Under *dq*-axis form, the active and reactive power, transferring from the VSC inverter, can be listed below [13, 24]

$$P_s = -\frac{3}{2}u_{sd}i_{sd} - \frac{3}{2}u_{sq}i_{sq} \qquad (6)$$

$$Q_s = \frac{3}{2}u_{sd}i_{sq} - \frac{3}{2}u_{sq}i_{sd} \qquad (7)$$

Where $i_{sd}$and $i_{sq}$are the *dq*-axis current components of the VSC, $u_{sd}$and u_{sq}represent the *dq*-axis voltage components at the PCC.

The equations of the VSC outer control loop in frequency domain can be acquired,

$$i_{sdref} = (k_{p1} + \frac{k_{I1}}{s})(u_{sd} - u_{sdref}) \qquad (8)$$

$$i_{sqref} = (k_{p2} + \frac{k_{I2}}{s})(u_{sq} - u_{sqref}) \qquad (9)$$

Where i_{sdref}&i_{sqref}denotes the *dq*-axis current references generated by the outer control loop, the command references of the *dq*-axis voltage components are given by [11]

ISSN (Print) : 2320 – 3765
ISSN (Online): 2278 – 8875

International Journal of Advanced Research in Electrical, Electronics and Instrumentation Engineering

(A High Impact Factor, Monthly, Peer Reviewed Journal)

Website: www.ijareeie.com

Vol. 7, Issue 5, May 2018

$$u_{sdref} = U_s^* , u_{sqref} = 0 \quad (10)$$

Where $U_s^*$is the nominal amplitude of the PCC voltage, the outer control loop of the inverter station is developed to control the angular frequency of the PCC voltage, setting the synchronizing signal as [22]

$$\begin{cases} \theta_{passive} = \int_{\tau=0}^{t} \omega^* \, d\tau + \theta_0 \\ \omega^* = 2\pi f^* \end{cases} \quad (11)$$

$f^*$is the command reference of the frequency of the PCC voltage considering it as 50 Hz.

III. IMPROVED CONTROL STRATEGY

Therefore to improve the voltage stability of the passive industrial network, this section presents two major ride-through methods, which comprise of a modified current control strategy (MCCS) and a frequency hysteresis control (FHC). These are designed based on the conventional ac voltage control (CAVC) with VSC at the receiving end.

3.1 Modified Current Limit Strategy:

In orthodox power systems, the reactive power flow and the ac voltage are connected closely because of the inductive characteristics of high voltage transmission lines. The variation of reactive power in the system may have a high effect on the ac voltage of the power grid [23]. When, the VSC-HVDC is delivering to passive industrial loads, the rectifier station works on the dc voltage control mode. In case of faults in the sending side, there is an ac voltage drop in the grid and the current of the VSC rectifier reaches the limit. As a result, the VSC at the grid end is incapable to uphold the dc voltage. The change of the active power may cause deviations in the dc voltage, causing a disturbance of the ac voltage at the PCC; meanwhile the ac voltage in the passive system is modulated from the dc voltage of the VSC-HVDC [22]. Thus, during severe faults, the active power will have high impact on the ac voltage of the passive industrial installations. Alternatively, the reactive power is still critical for the voltage stability of the passive system. Therefore, an analysis should be done to investigate that whether the active power or the reactive power is responsible for the deviation of the ac voltage at the receiving end.

The active and reactive power sending out from the VSC at the receiving side can be listed below

$$P = \frac{U_s U_c}{X} sin\delta \quad (12)$$

$$Q = \frac{U_c(U_c - U_s cos\delta)}{X} \quad (13)$$

Where $U_s$and $U_c$are the amplitude of the PCC and the VSC voltage, X denotes the equivalent reactance connecting the PCC and the VSC inverter as shown in Fig. 1. In practice, the equivalent resistance (R) is much smaller than the equivalent reactance (X) [27]. So, the equivalent resistance is ignored in (12) and (13).

$$P^2X^2 + Q^2X^2 = U_s^2U_c^2 + 2QXU_c^2 - U_c^4 = (U_s^4 + 2QXU_c^2)k^2 - k^2U_s^4 \quad (14)$$

Where $k = \frac{U_c}{U_s}$

ISSN (Print) : 2320 – 3765
ISSN (Online): 2278 – 8875

International Journal of Advanced Research in Electrical, Electronics and Instrumentation Engineering

(A High Impact Factor, Monthly, Peer Reviewed Journal)

Website: www.ijareeie.com

Vol. 7, Issue 5, May 2018

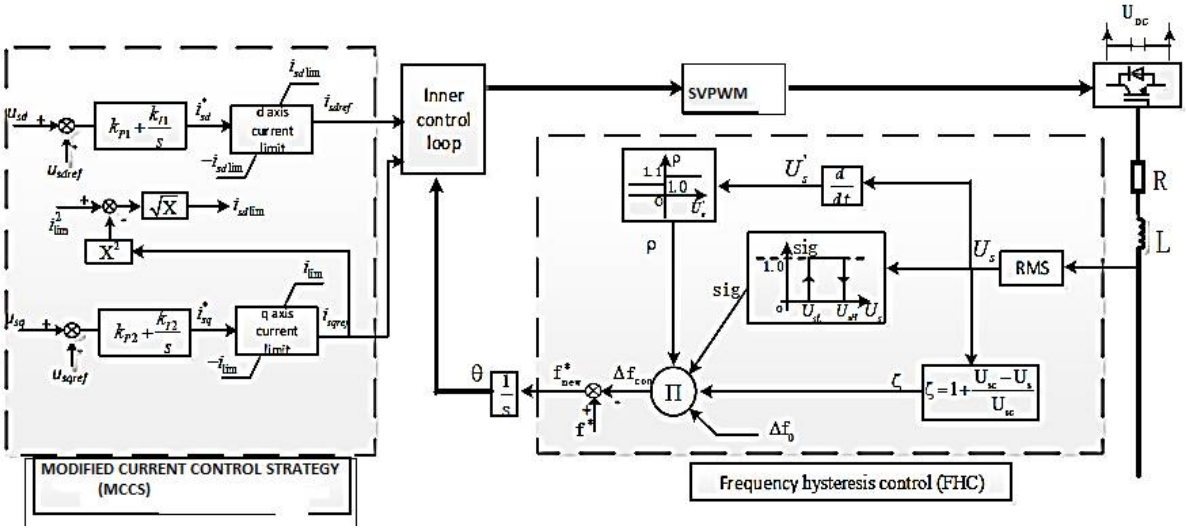

Fig. 4 Block diagram of proposed control method of the VSC-HVDC at the receiving side.

In the block diagram shown in Fig. 1, a metallic three-phase fault is simulated at the sending end of the VSC-HVDC. The fault is applied at 0.5 s and is cleared at 0.6 s. Fig. 5 shows the variations of the ratio of $U_C$and U_S(i.e. k). From Fig. 5, in steady state conditions, the value of k is nearly 1.06. In the fault period, the value of k ranges between 0.898~1.116.

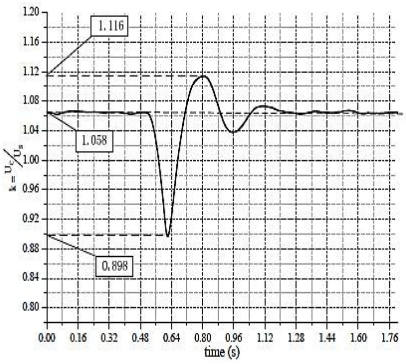

Fig.5.The characteristics of k during fault.

From (14), the expression of $U_S$is derived as

$$U_S = \sqrt{\frac{a_1 \pm \sqrt{4k^2X^2a_2}}{2k^2(k^2-1)}} \qquad (16)$$

$$a_1 = 2k^2XQ \qquad (17)$$

$$a_2 = Q^2 + (1-k^2)P^2 \qquad (18)$$

From (17), we can know that $a_1$is proportional to Q, which means that $a_1$is decided by the reactive power. In (18), the coefficient of $P^2$is $(1-k^2)$ and the coefficient of $Q^2$is 1.0. Since the range of k is 0.898~1.116, the ratio of $(1\text{-}k^2)$

ISSN (Print) : 2320 – 3765
ISSN (Online): 2278 – 8875

International Journal of Advanced Research in Electrical, Electronics and Instrumentation Engineering

(A High Impact Factor, Monthly, Peer Reviewed Journal)

Website: www.ijareeie.com

Vol. 7, Issue 5, May 2018

varies from 0.0 to 0.24. Therefore, a_2 is mainly affected byQ^2, that denotes the key factor that affects $a_2$is also reactive power. Hence, it is found thatU_s, the amplitude of the PCC Voltage is mainly determined by the reactive power. Thus, during severe faults, it's important to give priority to the need of the reactive power, which can improve the voltage stability of the passive industrial system efficiently. From Fig. 4, ac voltage controller is used in the inverter of the VSC-HVDC system. As presented in Fig. 6a, in steady conditions, $u_{sq}$is 0 and u_{sd}equals U_s, the amplitude of the PCC voltage. According to (7), it is derived that the reactive power is mainly judged by i_{sq}in steady conditions. When, a severe fault occurs at the grid end, the active power transmitting to the industrial system falls, which may lead to a drop of the dc voltage. Since the ac voltage in the passive industrial system is modulated from the dc voltage of the VSC-HVDC, the inverter VSC produces an output voltage (U_c) with the limited amplitude and the specified frequency. Once the fault occurs, the ac current in the passive industrial system won't change quickly due to the inductance of induction motors and the equivalent inductance connecting the PCC and the VSC inverter [29]. Thus, it is presented in Fig. 6b that when the fault occurs, the voltage of the equivalent impedance connecting the PCC and the VSC inverter (i.e., the ΔU in Fig. 6) is nearly the same as that in steady operation and the phase angle of $U_s$lags behind the *d* axis whoserotational speed is set by the synchronizing signal in equation (11). This will result in a decrease of the PCC frequency. Due to the fast response of the VSC controller which aims to make the u_{sq}equal to 0 [27], the U_s will try to align to the *d* axis and the phase angle θ (see Fig. 6b) amid U_s and the *d* axis is rather small during the dynamic process. The *q*-axis voltage component at the PCC is

$$u_{sq} = U_s \cos\left(\boldsymbol{\theta} + \frac{\boldsymbol{\pi}}{\mathbf{2}}\right) = -U_s sin\boldsymbol{\theta} \qquad (19)$$

It is derived from (19) that in transient condition, the value of $u_{sq}$is negative and relatively small. Note that in (7), u_{sq} is the coefficient of i_{sd}in the expression of *Q*. Thus, during disturbances, i_{sd} has a small impact on the *Q* and $i_{sq}$is still the main factor that affects the reactive power. Because the reactive power is mainly decided by i_{sq}in steady and transient conditions, the MCCS that gives priority to meeting the setting of $i_{sq}$is proposed as

$$i^*_{sd\ lim} = \sqrt{i^2_{lim} - i^2_{sqref}}\ , \quad i^*_{sq\ lim} = i_{lim} \qquad (20)$$

Where $i_{lim}$is the VSC current limit, which is generally set as 1.1 times the total load. The$i_{sdlim}$is determined according toi_{sqref}, the new *q* axis current component, produced from the MCCS and the maximum VSC current. Fig.4 represents the control block of the MCCS.

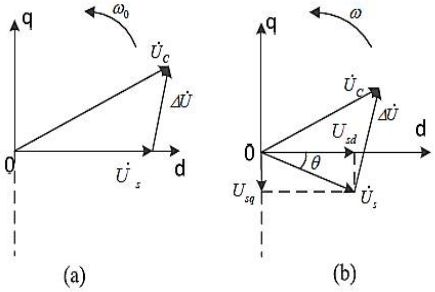

Fig. 6 The position ofU_s, $U_c$and the dq axis. (a) in the steady condition. (b) when the fault occurs at the grid end.

The idea of the MCLS is to raise i_{sq}, the *q* axis current component, during the fault period. It is noted that if the coefficient of i_{sq}in (7) (i.e., u_{sd}) can be increased in the transient conditions, the MCCS will have a better control result. Hence, an additional frequency control is given in the next section, which can decrease the absolute value of $u_{sq}$and increase the u_{sd}during faults. In this manner, more reactive power can be transmitted to the passive industrial installations and the ac voltage stability of the passive industrial system will have a further enhancement.

ISSN (Print) : 2320 – 3765
ISSN (Online): 2278 – 8875

International Journal of Advanced Research in Electrical, Electronics and Instrumentation Engineering

(A High Impact Factor, Monthly, Peer Reviewed Journal)

Website: www.ijareeie.com

Vol. 7, Issue 5, May 2018

3.2 Frequency Hysteresis Control:

The main purpose of the FHC is to produce a new reference frequency of the VSC output voltage based on the measurement of the ac voltage at the PCC. As the voltage drops, the FHC drops the set frequency $f^*$of the VSC at the receiving end spontaneously. It is derived by this means, the phase angle θ between U_s and the d axis (see Fig. 6b) will become smaller, which in turn can reduce the absolute value of u_{sq}also the MCCS can have a better control output. According to (9), in the fault period, the reduction of the variation of u_{sq}can also increasei_{sq}, the q axis current component, also increases the reactive power output generated by the VSC at the receiving end. Fig. 4 shows the FHC for the inverter of the VSC-HVDC. Whereas for the faults in the grid, the ac voltage of the passive system drops. When the amplitude of the ac voltage at the PCC is smaller than the starting voltageU_{sL}, the frequency controller is started and the signalin Fig. 4 is set as 1. The starting criterion is expressed as

$$U_s < U_{sL} \qquad (21)$$

When ac voltage at the PCC returns to a normal level, i.e., $U_s$is higher than the voltage limitU_{sH}, the FHC is removed and the *sig* in Fig. 4 is set as 0. The ending criterion is expressed as

$$U_s > U_{sH} \qquad (22)$$

From (23-25), the control parameters of the FHC are determined. From the equations, f^*_{new}produced by the FHC controller is the new set frequency of the VSC outer control loop. $\Delta f_0$is the basic control parameter in the FHC, which mostly depends on the ability of the passive network to bear the frequency deviations. If the induction motors in the passive network are sensitive to frequency disturbances, the value ofΔf_0will set to smaller. This value is set according to types of induction motors in the passive network. ζ is the penalty factor and $U_{sC}$is the control parameter used to calculate theζ. When the amplitude of the ac voltage $U_s$is lower thanU_{sC}, the ζ is set to greater than 1.0, which can further reduce the set frequency of the VSC at the receiving end. By this means, the θ in Fig. 6b will be small and there will be a further decrease in the absolute value ofu_{sq}. On the contrary, when$U_s$is higher thanU_{sC}, the ζ is fixed smaller than 1.0. In this paper, so as to mitigate the effect of removing the FHC $U_{sC}$is set to smaller than the voltage limitU_{sH}. As a result, when the FHC is removed, the set frequency of the VSC is smaller thanΔf_0. When there are more induction motors in the passive network or when the duration of severe faults is quite long, the values of $U_{sL}$and U_{sC}can be increased in order to further decrease the frequency of the VSC output voltage and increase the VSC output reactive power in transient conditions. ρ is the additional control parameter. When the rate of *Us* changes (i.e. dU_s/dt) is negative, which means the voltage in the passive system is continuing to fall, ρ is set to greater than 1.0. In this paper, the value is set as 1.1. When dU_s/dt is positive, ρ is set as 1.0.

$$f^*_{new} = f^* - \Delta f_{con} \qquad (23)$$

$$\Delta f_{con} = \rho\zeta\Delta f_0 \qquad (24)$$

$$\zeta = 1 + \frac{U_{sC}-U_s}{U_{sC}} * 100\% \qquad (25)$$

IV.SIMULATION AND RESULTS

From the topology in Fig. 1, the paper takes the test system in PSCAD/MATLAB to check the possibility of the control strategies proposed. By simulation, the VSC at the sending end runs on the dc voltage control mode and the reactive power control mode. An ac voltage controller is used on the inverter of the VSC-HVDC system. The constraints of the VSC-HVDC system are presented in Table I in the appendix. The VSC current limit (i_{lim}) is set to 1.1 times the total load [24]. As it is in Fig. 1, the industrial installations comprises of a static load and an induction motor IM which represents that majority of loads are induction motors in the passive system. All loads are connected to

ISSN (Print) : 2320 – 3765
ISSN (Online): 2278 – 8875

International Journal of Advanced Research in Electrical, Electronics and Instrumentation Engineering

(A High Impact Factor, Monthly, Peer Reviewed Journal)

Website: www.ijareeie.com

Vol. 7, Issue 5, May 2018

the PCC. The active and reactive powers consumed by the static load are 0.9 MW and 0.45 Mvar, correspondingly. Where, the ratio between induction motors and static loads is 19:1. Simulation data show that in the passive network, when the percentage of IM loads is higher than 58%, the ac voltage collapse occurs earlier than the dc voltage collapse during severe faults. It can be derived that in the case of induction motors account for more than 58% of all passive loads, the proposed control methods are appropriate. The defined parameters of the induction motor IM are listed in Table II in the appendix.

The control parameters of the FHC are set as U_{sL}=0.85 p.u,U_{sH} = 0.95 $p.u$,U_{sC}=0.7 p.u. andΔf_0=0.5 Hz. Where, the fault time is set as 0.1 s. With the increase of the fault time, a dc voltage collapse may occur and the passive industrial system becomes unstable certainly [6]. With the change of PWM techniques the Total Harmonic Distortion factor (THD) can vary in which SVPWM is adopted in this paper which reduces THD effectively.

Single-Phase Fault at the Sending Side:

Among all AC faults, single-phase ground fault is the most common fault. To test the fault ride-through capability of the control strategies, a single-phase fault is applied to the sending side of the VSC-HVDC at 0.5 s, when the system is under the steady state. After 0.1 s, the fault is cleared. The simulations have been done under different control strategies used on the inverter of the VSC-HVDC system, i.e., the conventional ac voltage control (CAVC), the CAVC with the MCCS and the CAVC with the MCCS and FHC. The simulation results are shown in Figs. 7~8. Fig. 7a shows the effects of the MCCS. When the inverter VSC is under the CAVC controller, the ac voltage at the PCC does not return to its pre-fault level after the fault clearance. While with the MCCS, the PCC voltage can keep stable after the fault. As shown in Fig. 7b~c, during the fault, the delivered active power reduces, which results in the decrease of the dc voltage. There are double frequency oscillations in the dc voltage during the single-phase fault. It could be observed from Fig. 7d that during this ac fault, the frequency of the voltage at the PCC drops because the phase angle ofU_s changes. As shown in Fig. 7e, the three controllers are able to keep the VSC current within the limit, which is set 1.1 times the total load. Figs. 7f~h show dynamic performances of the q axis current, voltage components at the PCC and the reactive power transferred from the VSC inverter. It could be observed from Fig. 7f that during the period of the single-phase fault, the value of the$u_{sq}$is relatively small. Thus, the reactive power Q is mainly affected by i_{sq}. It is denoted that with the FHC, the change of the u_{sq}at the PCC gets smaller in the transient condition, which can enhance the control of the MCCS and increase the value of the i_{sq} (see Fig. 7g).

As shown in Fig. 7h, there will be a more increase of the reactive power transmitted from the VSC inverter. The effect of the FHC is clearly presented in Fig. 7a. When the FHC is added to the VSC controller, the ac voltage at the PCC increases by 0.15 p.u. during the ac fault and returns back to 1.0 p.u. more quickly after the fault clearance. From the simulation results, it is derived that when the VSC at the receiving end adopts the CAVC controller with the MCCS and FHC, the voltage stability of the passive industrial system can be enriched more effectively. Fig. 8 gives the Induction motor(IM) responses of the single-phase fault. With the MCCS, the IM can ride through the ac fault. As in Fig. 7d, with the FHC, the frequency at the PCC drops lower as compared with the other controllers. This result in the decrease of the consumed active power of the IM [15] (see Fig. 8a). Thus, as shown in Fig. 7b~c, the drop of the dc voltage is smaller with the FHC.

ISSN (Print) : 2320 – 3765
ISSN (Online): 2278 – 8875

International Journal of Advanced Research in Electrical, Electronics and Instrumentation Engineering

(A High Impact Factor, Monthly, Peer Reviewed Journal)

Website: www.ijareeie.com

Vol. 7, Issue 5, May 2018

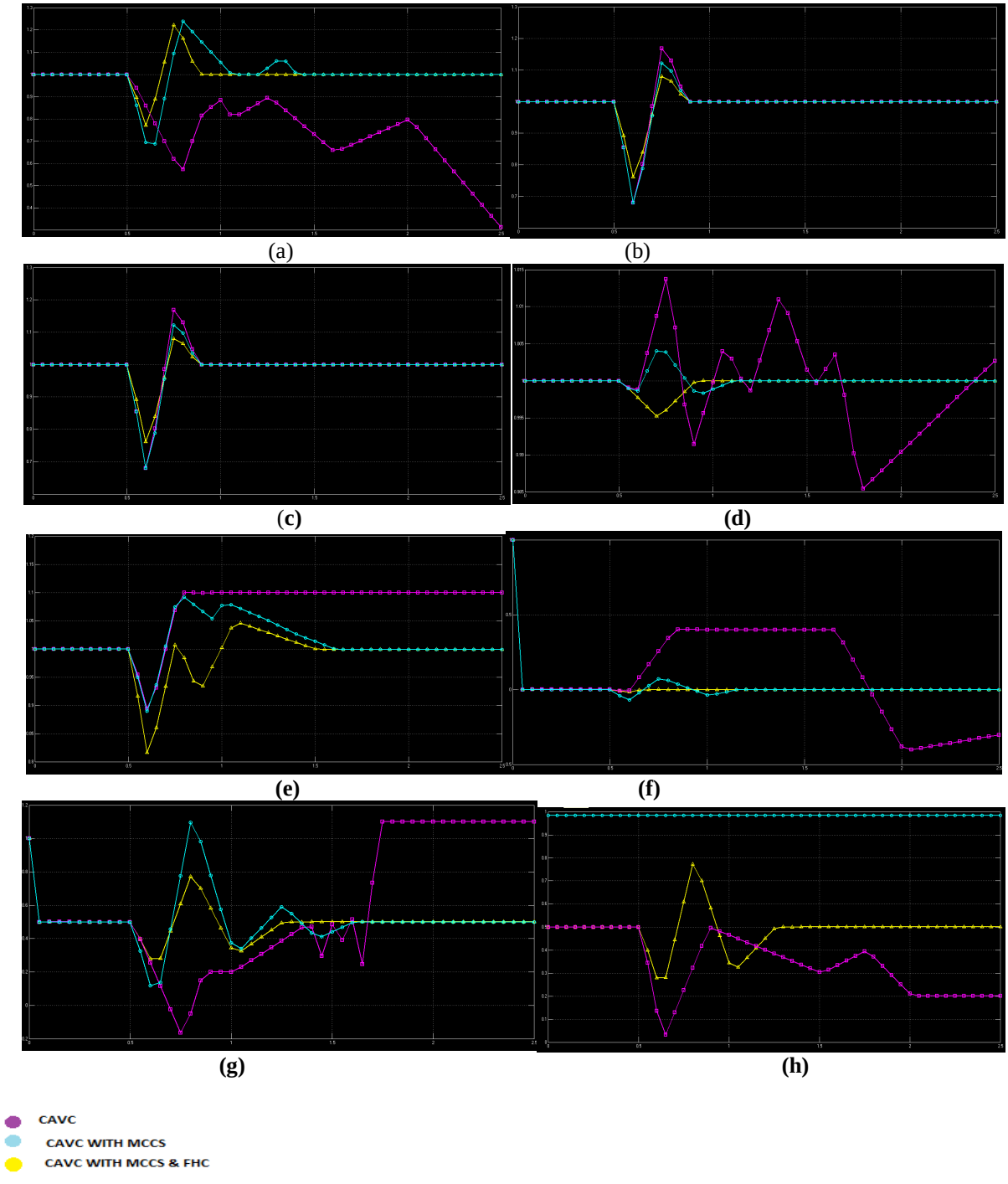

Fig. 7 System responses of single-phase fault with different control methods. (a) ac voltage at the PCC. (b) dc voltage of the rectifier VSC. (c) dc voltage of the inverter VSC. (d) Frequency of the passive system. (e) VSC current. (f) The q

ISSN (Print) : 2320 – 3765
ISSN (Online): 2278 – 8875

International Journal of Advanced Research in Electrical, Electronics and Instrumentation Engineering

(A High Impact Factor, Monthly, Peer Reviewed Journal)

Website: www.ijareeie.com

Vol. 7, Issue 5, May 2018

axis component of voltage at the PCC. (g) The q axis current component of VSC. (h) Reactive power transferred from the VSC inverter.

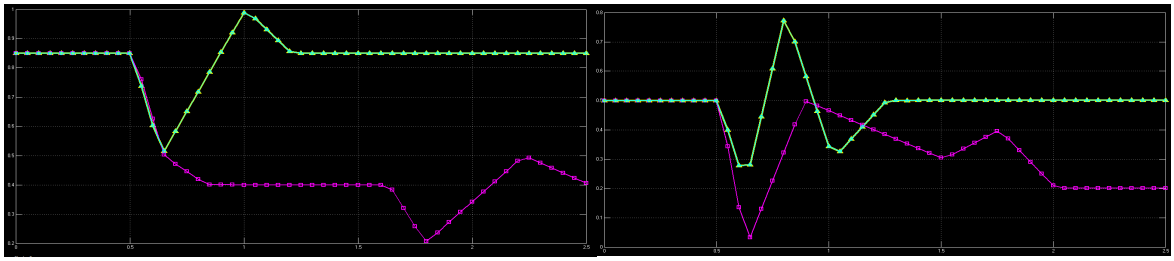

(a) **(b)**

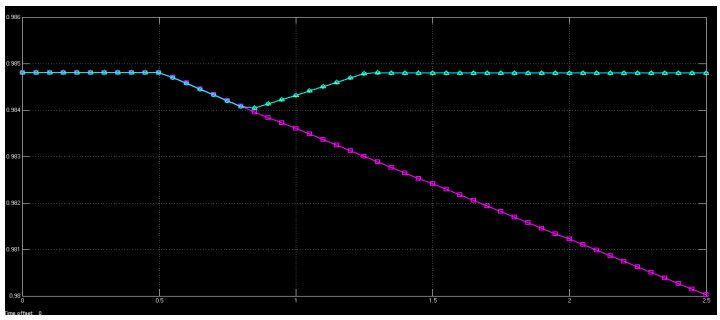

(c)

Fig. 8 IM responses of the metallic single-phase fault with different control methods. (a) IM active power. (b) IM reactive power. (c) IM speed.

Similarly, for the metallic three phase to ground faults are shown in figures 9 & 10.

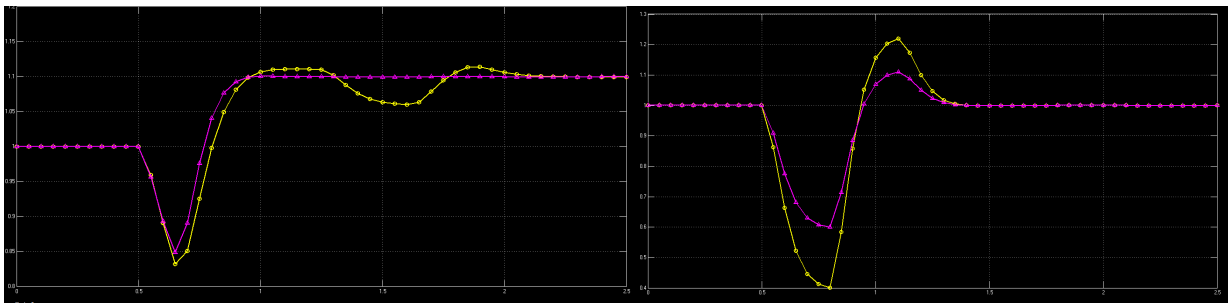

(a) **(b)**

ISSN (Print) : 2320 – 3765
ISSN (Online): 2278 – 8875

International Journal of Advanced Research in Electrical, Electronics and Instrumentation Engineering

(A High Impact Factor, Monthly, Peer Reviewed Journal)

Website: www.ijareeie.com

Vol. 7, Issue 5, May 2018

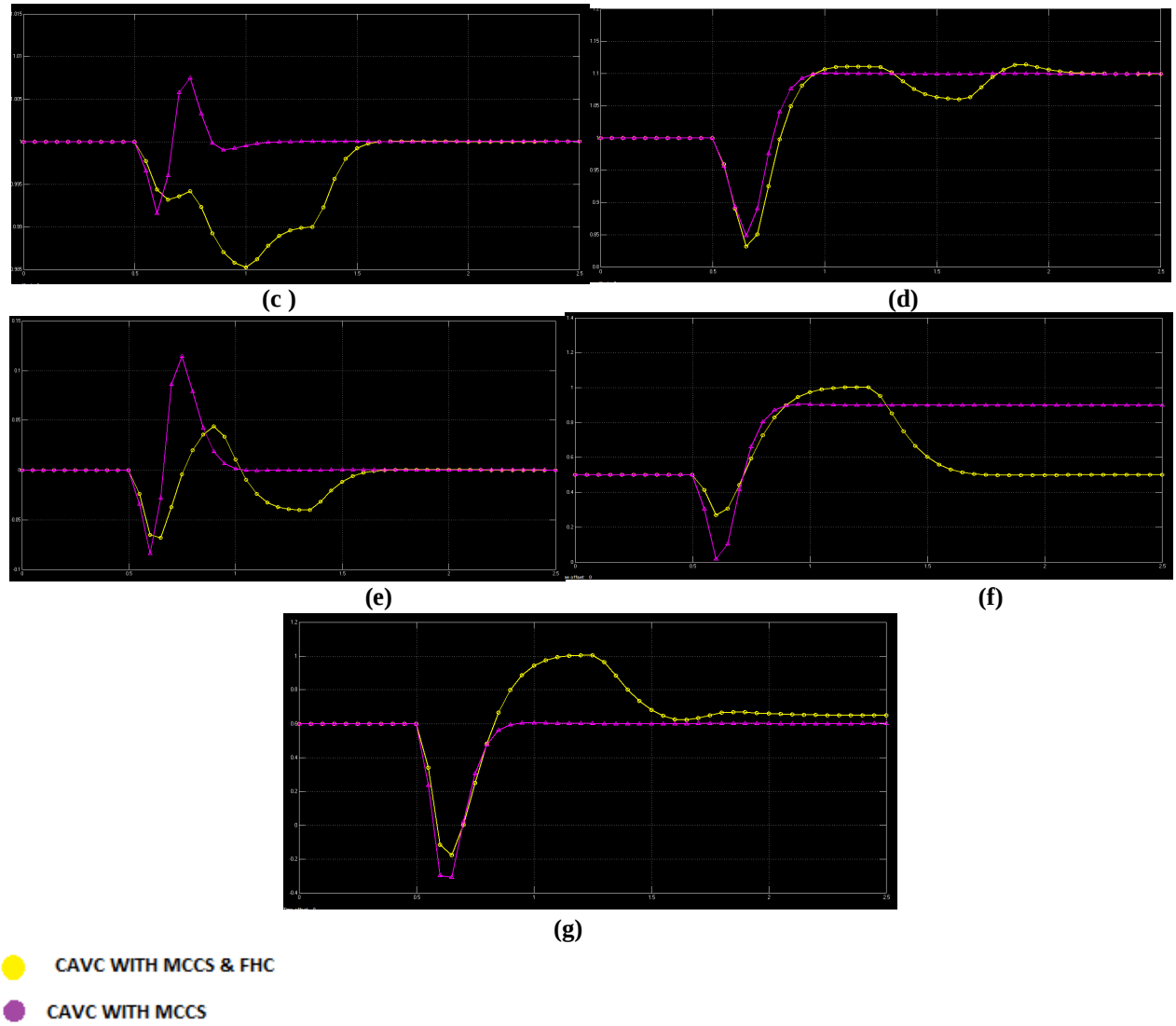

Fig. 9 System responses of the metallic three-phase fault with and without the FHC. (a) ac voltage at the PCC. (b) dc voltage of the inverter VSC. (c) Frequency of the passive system. (d) VSC current. (e) The q axis component of voltage at the PCC. (f) The q axis current component of VSC. (g) Reactive power transferred from the VSC inverter.

ISSN (Print) : 2320 – 3765
ISSN (Online): 2278 – 8875

International Journal of Advanced Research in Electrical, Electronics and Instrumentation Engineering

(A High Impact Factor, Monthly, Peer Reviewed Journal)

Website: www.ijareeie.com

Vol. 7, Issue 5, May 2018

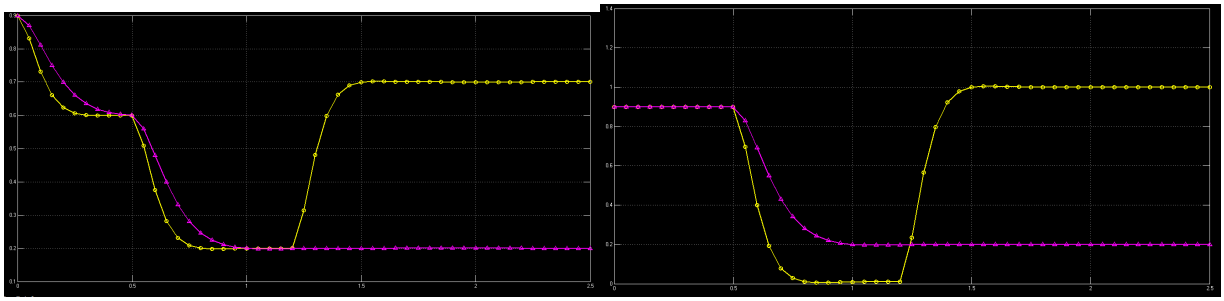

(a) **(b)**

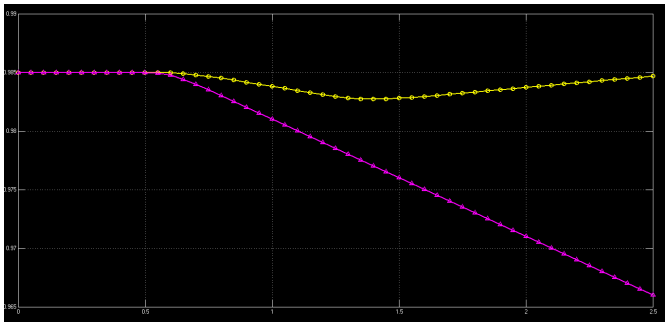

(c)

Fig. 10 IM responses of the metallic three-phase fault with and without the FHC. (a) Consumed active power. (b) Consumed reactive power. (c)IM speed.

V.CONCLUSION

This paper is to design control strategies to improve the voltage stability of the VSC-HVDC based passive industrial installations. By the analytical result that the main cause influencing the ac voltage of the passive system is the reactive power, the control techniques that comprise of the modified current control strategy and the frequency hysteresis control are taken. The purpose of selecting the MCCS is that in steady state and transient conditions, the reactive power transmitted from the inverter of the VSC-HVDC is mostly decided by i_{sq}, the q axis component of the VSC current. When the MCCS is added to the outer control loop of the inverter, the setting of i_{sq}can be met better in order to increase reactive power output of the VSC. From MCCS basis, an additional frequency control is proposed. The purpose of the FHC is to reduce the set frequency of the VSC at the receiving end according to the measurement of the ac voltage in the passive industrial system. In this manner, the control effect of the MCCS can be enhanced. The decrease of the set frequency can lead to an increase of thei_{sq}, which in turn increases the reactive power output. The simulation verifications were carried out during a metallic single-phase fault and a metallic three-phase fault respectively. By studying the simulation results, it can be concluded that,1)when a metallic single-phase fault occurs at the sending end of the VSC-HVDC system, the ac voltage of the passive industrial system drops certainly. When the VSC at the receiving end is working on CAVC controller, the ac voltage does not fall back to its pre-fault level after the fault clearance. Whereas, with the MCCS the voltage will be stable after the fault clearance. The voltage stability can be improved further when the MCCS and FHC are added to the VSC controller accordingly. 2) During a metallic three-phase fault, the ac voltage in the passive system cannot keep stable under the VSC controller with the MCCS. While with the FHC, a voltage collapse is avoided, this means that it is likely to decrease the set frequency of the VSC at the receiving end to ride through severe faults. Since SVPWM technique is added to this control by which it reduces

ISSN (Print) : 2320 – 3765
ISSN (Online): 2278 – 8875

International Journal of Advanced Research in Electrical, Electronics and Instrumentation Engineering

(A High Impact Factor, Monthly, Peer Reviewed Journal)

Website: www.ijareeie.com

Vol. 7, Issue 5, May 2018

Total Harmonic Distortion (THD) to some margin. Hence from above, the control strategies proposed in this paper could improve voltage stability of the passive industrial installations efficiently.

VI. APPENDIX

CONTROL PARAMETERS

TABLE I

VSC-HVDC PARAMETERS

Rated DC voltage ($\boldsymbol{V_{dc}}$)	±20 kV
Modulation frequency	1350 Hz
Rated AC voltage ($\boldsymbol{U_s}$)	4.16 kV
Rated (base) apparent power	20 MVA
System frequency	50 Hz
Reactive power capacity of filter	0.05 p.u.
Dc capacitor $\boldsymbol{2C_{dc}}$	375 μF
VSC equivalent inductance (L)	0.00195H
VSC equivalent resistance (R)	0.0085Ω
k_{p1}, k_{I1}	6, 60.61
k_{p2}, k_{I2}	6, 34.48

TABLE II

INDUCTION MOTOR PARAMETERS

Rs+jXs(p.u.)	0.0018+j0.0806
Xm(p.u.)	2.820
Rr+jXr(p.u.)	0.0282+ j0.0936
S (%)	2.156
H(sec)	0.56
S(MVA)	19
V(kV)	4.16
Tm(p.u.)	0.8

REFERENCES

[1] Lamell, Jan O., Timothy Trumbo, and Tom F. Nestli. "Offshore platform powered with new electrical motor drive system." IEEE Industry Applications Society 52nd Annual, 2005.
[2] Kim, Tae-O., Hui-Dong Ju, and Gyu-Hong Kang. "Analysis of power system harmonics for an offshore design with VTB dynamic model." *IEEE Vehicle Power and Propulsion Conference*, 2012.
[3] McGranaghan, Mark F., David R. Mueller, and Marek J. Samotyj. "Voltage sags in industrial systems." *IEEE Transactions on industry applications*, vol. 29, no. 2, pp. 397-403, 1993.
[4] Melhorn, Christopher J., Timothy D. Davis, and George E. Beam. "Voltage sags: their impact on the utility and industrial customers." *IEEE Transactions on Industry Applications*, vol. 34, no. 3, pp. 549-558, 1998.
[5] Becker, Carl, et al. "Proposed chapter 9 for predicting voltage sags (dips) in revision to IEEE Std 493, the Gold Book." *IEEE Transactions on Industry Applications*, vol. 30, no. 3, pp. 805-821, 1994.
[6] C. Du, et al. "A new control strategy of a VSC–HVDC system for high-quality supply of industrial plants." *IEEE Transactions on Power Delivery*, vol. 22, no. 4, pp. 2386-2394, 2007.
[7] Flourentzou, Nikolas, Vassilios G. Agelidis, and Georgios D. Demetriades. "VSC-based HVDC power transmission systems: An overview." *IEEE Transactions on Power Electronics*, vol. 24, no. 3 , pp. 592-602, 2009.
[8] Y. Liu, and C. Zhe. "A flexible power control method of VSC-HVDC link for the enhancement of effective short-circuit ratio in a hybrid multi-in feed HVDC system." *IEEE Transactions on Power Systems*, vol. 28, no. 2, pp. 1568-1581, 2013.
[9] Chehardeh, M. Isapour, et al. "An optimal control strategy to alleviate sub-synchronous resonance in VSC-HVDC systems." *Power Electronics and Intelligent Transportation System (PEITS), 2009 2nd International Conference on*. Vol.1,2009.
[10] Feltes, Christian, et al. "Enhanced fault ride-through method for wind farms connected to the grid through VSC-based HVDC transmission." *IEEE Transactions on Power Systems*, vol. 24, no. 3, pp. 1537-1546, 2009.
[11] H. Chen, "Research on the control strategy of VSC based HVDC system supplying passive network," in *Power & Energy Society General Meeting*, 2009.
[12] S. Li, et al. "A study on VSC-HVDC based black start compared with traditional black start." *Sustainable Power Generation and Supply, 2009. SUPERGEN'09. International Conference on*. IEEE, 2009.

ISSN (Print) : 2320 – 3765
ISSN (Online): 2278 – 8875

International Journal of Advanced Research in Electrical, Electronics and Instrumentation Engineering

(A High Impact Factor, Monthly, Peer Reviewed Journal)

Website: www.ijareeie.com

Vol. 7, Issue 5, May 2018

[13] C. Guo, and Chengyong Zhao. "Supply of an entirely passive AC network through a double-infeed HVDC system." *IEEE Transactions on Power Electronics*, vol. 25, no. 11, pp. 2835-2841, 2010.
[14] Zhang L. Modelling and control of VSC-HVDC links connected to weak AC systems[D]. KTH，2010.
[15] C. Du, Evert Agneholm, and Gustaf Olsson. "Comparison of different frequency controllers for a VSC-HVDC supplied system." *IEEE Transactions on Power Delivery*, vol. 23, no. 4, pp. 2224-2232, 2008.
[16] W. He, et al. "Case Study of Integrating an Offshore Wind Farm with Offshore Oil and Gas Platforms and with an Onshore Electrical Grid." *Journal of Renewable Energy*, 2013.
[17] B. Liu, et al. "Faults mitigation control design for grid integration of offshore wind farms and oil & gas installations using VSC HVDC." *Power Electronics Electrical Drives Automation and Motion (SPEEDAM), International Symposium on*. IEEE, 2010.
[18] Haileselassie, Temesgen M., Marta Molinas, and Tore Undeland. "Multi-terminal VSC-HVDC system for integration of offshore wind farms and green electrification of platforms in the North Sea." *Helsinki University of Technology*, 2008.
[19] X. Tang, and Dylan Dah-Chuan Lu. "Enhancement of voltage quality in a passive network supplied by a VSC-HVDC transmission under disturbances." *International Journal of Electrical Power & Energy Systems*, vol.54, pp. 45-54, 2014.
[20] S. Liu, et al. "Electromechanical transient modelling of modular multilevel converter based multi-terminal HVDC systems." *IEEE Transactions on Power Systems*, vol. 29, no. 1, pp. 72-83, 2014.
[21] L. He, and Chen-Ching Liu. "Parameter identification with PMUs for instability detection in power systems with HVDC integrated offshore wind energy." *IEEE Transactions on Power Systems*, vol. 29, no. 2, pp. 775-784, 2014.
[22] M. Guan, Pan W, Zhang J,et al. "Synchronous Generator Emulation Control Strategy for Voltage Source Converter (VSC) Stations[J]." *IEEE Transactions on Power Systems*, vol. 99, pp. 1-9, 2015.
[23] P. Kundur, *Po*wer System Stability and Control. New York: Mc Graw-Hill, pp. 647-658, 1994.
[24] G. Tang, Z. Xu, H. Dong, et al, "Sliding Mode Robust Control Based Active-Power Modulation of Multi-Terminal HVDC Transmissions," IEEE Trans. Power Syst., vol. Early Access Online, 2015.
[25] G. Li, *et al*., "Modelling of VSC-HVDC and control strategies for supplying both active and passive systems," in Power Engineering Society General Meeting, 2006.
[26] M. Guan, Z. Xu, "Modelling and control of a modular multilevel converter-based HVDC system under unbalanced grid conditions". IEEE Transactions on Power Electronics, vol. 27, no. 12, pp. 4858-4867, 2012
[27] Z. Xu, et al. "Voltage source converter based high voltage direct current transmission system". Beijing：China Machine Express，2012：6(in Chinese).
[28] M. Guan, Z. Xu and H. Chen, "Control and modulation strategies for modular multilevel converter based HVDC system". IECON 2011-37th Annual Conference on IEEE Industrial Electronics Society. pp. 849-854, 2011
[29] S. Li, Z. Xu, et al. "Study on MMC-HVDC Switching Scheme Between Grid-Connected and Passive Islanding Mode." *Proceedings of the CSEE*，vol. 35, no. 9, pp. 2152-2161, 2015 (in Chinese).
[30] Mohammad Hussain Khan, Veeranjaneyulu Gopu "Fuzzy Logic Controller Based on Voltage Source Converter-HVDC with MMC Topology" in international journal for Modern Trends in Science and Technology, Volume: 2,Issue: 08,August 2016, ISSN: 2455-3778.